

Surface Coverage in Sensor Networks

Linghe Kong, *Member, IEEE*, Mingchen Zhao, Xiao-Yang Liu, Jialiang Lu, *Member, IEEE*, Yunhuai Liu, *Member, IEEE*, Min-You Wu, *Senior Member, IEEE*, and Wei Shu, *Senior Member, IEEE*

Abstract—Coverage is a fundamental problem in wireless sensor networks (WSNs). Conventional studies on this topic focus on 2D ideal plane coverage and 3D full space coverage. The 3D surface of a field of interest (FoI) is complex in many real-world applications. However, existing coverage studies do not produce practical results. In this paper, we propose a new coverage model called *surface coverage*. In surface coverage, the field of interest is a complex surface in 3D space and sensors can be deployed only on the surface. We show that existing 2D plane coverage is merely a special case of surface coverage. Simulations point out that existing sensor deployment schemes for a 2D plane cannot be directly applied to surface coverage cases. Thus, we target two problems assuming cases of surface coverage to be true. One, under stochastic deployment, what is the expected coverage ratio when a number of sensors are adopted? Two, if sensor deployment can be planned, what is the optimal deployment strategy with guaranteed full coverage with the least number of sensors? We show that the latter problem is NP-complete and propose three approximation algorithms. We further prove that these algorithms have a provable approximation ratio. We also conduct extensive simulations to evaluate the performance of the proposed algorithms.

Index Terms—Wireless sensor networks, surface coverage, expected coverage ratio, optimal coverage strategy

1 INTRODUCTION

COVERAGE problem is fundamental in wireless sensor networks (WSNs). Each sensor is deployed to sense a section of a field of interest (FoI). An FoI is considered fully covered if and only if every point on the surface is covered by at least one sensor. The quintessence of the coverage problem is to use the least number of sensors to satisfy specific service requirements, for example, coverage ratio, network connectivity, and robustness. Solutions to the coverage problem have important applications in base station deployment in cellular networks, coverage in wireless mesh networks and so on.

Existing works on coverage issues focus mainly on 2D plane coverage or 3D full space coverage. In 2D plane coverage [16], [3], sensors are only allowed to be deployed on an ideal plane. And, in 3D full space coverage [10], [26], the FoI is assumed to be the 3D full space where sensors can be positioned freely within the whole FoI.

In many real-world applications, however, the FoI is neither a 2D ideal plane nor a 3D full space. Instead, they are complex surfaces. For example, in the Tungurahua volcano monitoring project [1] (see Fig. 1), sensors are deployed on the volcano, which is a surface. Existing 2D plane coverage solutions do not provide a workable strategy. If the 2D uniform deployment is adopted, there will be some coverage dead zone on the complex surface as illustrated in Fig. 2 (we called coverage dead zone problem). Similarly, 3D full

space coverage solutions cannot be applied either, because sensors in this case can only be deployed on the exposed surface area, and not freely inside the volcano or in the air. Three-dimensional full space coverage solutions are not discussed in this paper because they differ fundamentally from issues of complex surface coverage.

To address the coverage solution in the surface applications, we propose an innovative model called surface coverage. The surface coverage in WSNs (complex surfaces) is superior to solutions derived from conventional 2D ideal plane and 3D full space coverage methodologies. Nonetheless, the advantages of surface coverage come with new challenges such as how to handle variations in the shape of the surface. This paper studies two problems in WSN surface coverage. One, computing the expected coverage ratio when a given number of sensors are scattered under stochastic deployment. Two, finding the optimal deployment strategy with guaranteed full coverage and the least number of sensors when sensor deployment is pre-determined. We prove that the optimum surface coverage problem is NP-complete when applied to complex surface. Then, we propose three approximation algorithms with a provable performance bound for coverage of complex surfaces. The methodology used in this paper can be extended to other issues in surface coverage, for example, connectivity problems and mobility problems.

The main results and contributions are summarized as follows:

- To our best knowledge, this is the first work to tackle the surface coverage problem in WSNs. We propose a new model for the coverage problem.
- We derive analytical expressions of the expected coverage ratio on surface coverage for stochastic deployment. Simulation experiments are conducted to verify the results.

- L. Kong, X.-Y. Liu, J. Lu, Y. Liu, M.-Y. Wu, and W. Shu are with the Shanghai Jiao Tong University, Room 121, No 3, SEIEE Building, Dong Chuan Road, Shanghai 200240, China. E-mail: linghe.kong@sjtu.edu.cn.
- M. Zhao is at Room 613, 3330 Walnut Street, Philadelphia, PA, 19104.

Manuscript received 23 May 2012; revised 23 Jan. 2013; accepted 26 Jan. 2013; published online 14 Feb. 2013.

Recommended for acceptance by X.-Y. Li.

For information on obtaining reprints of this article, please send e-mail to: tpds@computer.org, and reference IEEECS Log Number TPDS-2012-05-0489. Digital Object Identifier no. 10.1109/TPDS.2013.35.

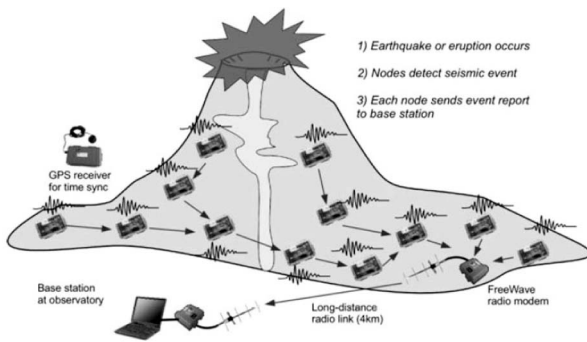


Fig. 1. A case study of the volcano monitoring project by Harvard Sensor Networks Lab [1], which is a typical surface coverage.

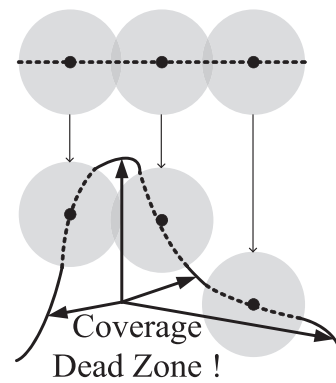


Fig. 2. The coverage dead zone problem occurs when the traditional 2D plane solution “uniform distribution” is directly adopted on a 3D surface (side view).

- We formalize the planned deployment problem and prove that it is NP-complete. Three approximation algorithms are proposed with provable approximation performance.
- We build the problem scope of surface coverage, which includes diverse dimensions. We also discuss the availability of our methods in different type of FoIs, sensors, distributions, and other requirements.

The remainder of the paper is organized as follows: In Section 2, we summarize the related works. In Section 3, we discuss the assumptions and models used throughout the paper. In Section 4, we present the analytical results of the expected coverage ratio under stochastic deployment. In Section 5, we describe the solution to the optimum deployment strategy under planned deployment. We evaluate our results in Section 6. We discuss some practical issues in Section 7. Section 8 concludes the paper. In the supplemental material, which can be found on the Computer Society Digital Library at <http://doi.ieeecomputersociety.org/10.1109/TPDS.2013.35>, Section 1 gives the detailed proofs of all theorems in this paper and Section 2 extends our method to other cases in the problem scope.

2 RELATED WORK

2.1 Coverage of the 2D Plane and the 3D Space

There are several ways to classify existing research on the coverage problem. One is the type of FoI: 2D ideal plane FoI [22], [13], [18], [25], [20], [6], [16], [11], [17], [7], [4], [24], [5], [3] or 3D full space FoI [10], [26]. Early work on coverage for the 2D ideal plane assumed that the plane was infinite so as to avoid the edge effect [20], [16], [11], [3], but recent findings have shown these results to be impractical and offer tentative solutions to finite areas [17], [4]. As yet, fundamental problems for these finite areas remain unanswered (e.g., optimum coverage policy and mobile coverage), and coverage solutions for the 2D ideal plane continue to incite heated debate [24], [3]. Still, proposed solutions to the 2D ideal plane problem have found a wide range of applications and some of them are easily applied to the case of 3D full space. All of these results, derived from the 2D plane and then applied to 3D complex surface, suffer from the Coverage Dead Zone Problem.

Another way to classify existing work is by the type of sensors. Some early works assumed that sensors were static and homogeneous. More recent work began to consider

mobile sensors [20], [24], [15] and heterogeneous sensors [17]. For example, mobile sensors were employed to cover a certain area so that fewer static sensors were needed [20], [24]. Lazos and Poovendran [17] applied a new mathematical tool called “Integral Geometry” to solve the coverage problem when sensors are heterogeneous. Parts of our results are extended from the results from this work [17].

A third way to classify previous research is based on the deployment scheme. A deterministic scheme [11], [3] is a planned deployment (e.g., manual deployment [8]) that needs fewer sensors to cover a given area but is more time-consuming and labor intensive. Another deployment scheme is by stochastic or random deployment, which is advocated in [20], [17], [4], and [24]. This method deploys sensors by vehicles or aircraft. We consider both of these cases.

Also, there is other work that focuses on joint optimum coverage goals. Cardei et al. [6] proposed a scheduling policy to maximize the lifetime while covering. Kar and Banerjee [13] studied the relation between sensing coverage and communication connectivity. And in works [11], [3], the optimum coverage patterns for an ideal infinite plane with designated connectivity requirements were proposed. In particular, the recent barrier coverage [16], [7], [4] considered intrusion detection in a barrier area, which is quite different from traditional 2D plane coverage. All these works are, however, based on the 2D ideal plane and no complex surface in 3D space has yet been considered.

2.2 Coverage of the 3D Surface

Currently, several works started to study the surface coverage problem.

A distributed algorithm [27] was proposed to produce a triangulation for any arbitrary 2D and 3D sensor networks. Further, Jin et al. [12] studied the optimal solution for 3D surface sensor deployment with minimized overall unreliability. It also designed a series of excellent algorithms for practical implementation. This study focused on the homogeneous sensors with the deterministic deployment.

Liu and Ma [21] derived the expected coverage ratios for regular terrains by cone/cos model and for irregular terrains by digital elevation model. This work assumed that homogeneous sensors are stochastically deployed.

Compared with the recent works, in our paper, we build the problem scope of surface coverage, which includes

TABLE 1
Notations and Terms in Section 3

Symbol	Definition
SP3	Space surface Poisson point process model;
PP3	Planar surface Poisson point process model;
OSCP	The optimum surface coverage problem;
S	The bounded area of the 3D surface;
P	A set of points (positions in S) to deploy sensors;
$g^*(P)$	The union set of the coverage area if sensors are deployed at P ;
C	A feasible solution of P meets OSCP.

different type of FoIs, sensors, distributions, and other requirements. Our analysis methods and algorithms could be extended to these various dimensions.

3 PROBLEM STATEMENT

In this section, the problem scope of surface coverage is described. Then, sensor, surface, and distribution models are formulated. This is followed by a formal statement of the surface coverage problem in WSNs. And a brief summary of integral geometry and the Poisson point process are presented. Some notations and terms used in this section are listed in Table 1.

3.1 Problem Scope

The problem scope of surface coverage can be divided into several dimensions.

- The type of FoI:
 - The FoI is a bounded (finite) surface in 3D space.
 - The FoI has or has no hole on the surface.
- The type of sensors:
 - The sensors are static or mobile.
 - The sensing areas of all sensors are homogeneous or heterogeneous.
- The type of sensor distribution: deterministic deployment or stochastic deployment.
- The coverage requirement:
 - Full coverage or multiple coverage.
 - Coverage with or without the consideration of connectivity.

Throughout the main parts of this paper, we study the case that the FoI is a finite surface in 3D space without hole, the sensors are static and their sensing areas are homogeneous, both deterministic and stochastic deployment are studied, and the requirement is full coverage without connectivity limitation. In Section 2 of the online supplemental material, we extend our method to other cases in the problem scope.

3.2 Sensor Models

We assume that all sensors have the same sensing radius r in 3D Euclid space. They are statically deployed and stationary after deployment. A point is said to be *covered* by a sensor if it is located within the sensing area of the sensor. The FoI is, thus, partitioned into two regions: the

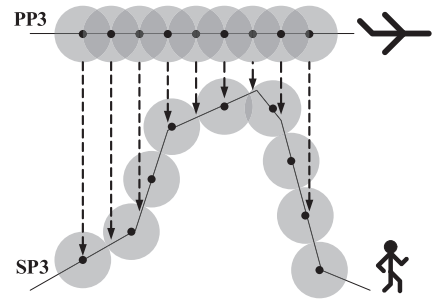


Fig. 3. The difference between PP3 and SP3 models.

covered region, which is covered by at least one sensor and the *uncovered region*, which is the complement of the covered region.

3.3 Surface Models

The surface can be expressed as $z = f(x, y)$ in a Cartesian coordinate system, which is considered the *reference system* for this surface. We assume that the FoI is convex, i.e., $z = f(x, y)$ is a single valued function. A surface is a *plane* if and only if the function is $z = c$ where c is a constant. A surface is a *slant* if and only if the function is $z = ax + by + c$ where a, b, c are constants. A sensor is said to be placed on the surface if its position lies on the surface. In this paper, we consider the FoI to be finite for practice. Thus, the boundary effect will be taken into account in all our calculations.

3.4 Sensor Distribution Models

Definition 3.1. The Z-projection of a point in 3D space is its projection point along the Z-axis on the xOy plane in the reference system, i.e., if the Cartesian coordinates of a point is (x, y, z) , the coordinates of its projection is $(x, y, 0)$. The Z-projection of a set in 3D space is a planar point set in xOy plane, which contains all the Z-projection points in the set.

For stochastic deployment, we consider two sensor distribution models. One is the *space surface Poisson point process model (SP3)* and the other is the *planar surface Poisson point process model (PP3)*.

- SP3 is described as $p_m = \frac{(\rho F)^m}{m!} e^{-\rho F}$.
- PP3 is described as $p_m = \frac{(\rho F')^m}{m!} e^{-\rho F'}$.

Where p_m is the probability that there are exactly m sensors on an FoI, where F is the area of the surface FoI, and F' is the Z-projection area of the FoI. It can be seen that both models agree with the traditional distribution model (i.e., Poisson point process) when the surface is an ideal plane.

Fig. 3 illustrates the difference between SP3 and PP3 models from a side view. The SP3 model is used to describe that sensors are deployed by humans or vehicles running on the surface. Hence, the sensors follow the Poisson distribution according to the surface. The PP3 model is used to describe that sensors are deployed by aircraft. The scattered sensors follow the Poisson distribution according to the flight path. Fig. 3 shows a typical example: nine sensor nodes (SP3) are isometric according to the surface, while the nodes (PP3) are isometric according to the flight

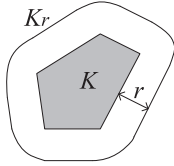


Fig. 4. An example of a parallel convex set.

line. When the nodes (PP3) drop along with the arrows, the deployed positions by two models are different.

3.5 Problem Statements

Definition 3.2. Let $z = f(x, y)$ be a surface S in 3D space. Let $\|S\|$ be the area of the surface S . The function $g : S \rightarrow 2^S$ is a function defined on the surface. Its value is the point set which is covered by sensor when the independent variable is the position of the sensor. The function $g^* : 2^S \rightarrow 2^S$ is a set function defined as $C \subseteq S$, $g^*(C) = \bigcup_{t \in C} g(t)$.

Simply, the function $g(P)$ describes the coverage area of a sensor if it is deployed at position P on the surface, when P has only one point. $g^*(P)$ presents the union set of the coverage area of sensors if they are deployed at positions P , when P is a set of points.

Definition 3.3. The coverage ratio is defined as: Given a point set $P (P \subseteq S)$, the coverage ratio f_c is a real value expressed as

$$f_c = \frac{\|g^*(P)\|}{\|S\|}. \quad (1)$$

Because f_c depends on the deployment of sensors P , we focus on the expected value of the coverage ratio $E(f_c)$ when P follows some distribution.

Definition 3.4. A feasible solution to the coverage problem is defined as a point set C that satisfies $C \subseteq S$, $g^*(C) \supseteq S$. The optimum surface coverage problem (OSCP) is defined as: minimize $|C|$, C is a feasible solution.

3.6 Integral Geometry and Poisson Point Process

Lemma 3.1. The Z-projection of a convex set C in 3D space is a planar convex set.

Definition 3.5. Parallel convex sets. The parallel set K_r , in the distance r of a convex set K is the union of all closed circular disks of radius r , the centers of which are points of K . The boundary ∂K_r , is called the outer parallel curve of ∂K in the distance r .

Fig. 4 gives an example of a parallel convex set.

Lemma 3.2. Let the area of the convex set K be F and perimeter of the convex set be L . Then the area F_r and perimeter L_r of the parallel convex set K_r is as follows:

$$F_r = F + Lr + \pi r^2, \quad (2)$$

$$L_r = L + 2\pi r. \quad (3)$$

Definition 3.6 (Poisson Point Process). Let \mathcal{D}_0 , \mathcal{D} be two domains of the plane such that $\mathcal{D} \subseteq \mathcal{D}_0$. Let F_0 , F be the areas of \mathcal{D}_0 , \mathcal{D} . According to the density $dP = dx \wedge dy$, the probability that a random point of \mathcal{D}_0 lies in \mathcal{D} is F/F_0 . If

there are n points chosen at random in \mathcal{D}_0 , the probability that exactly m of them lie in \mathcal{D} is a binomial distribution

$$p_m = \binom{n}{m} \left(\frac{F}{F_0}\right)^m \left(1 - \frac{F}{F_0}\right)^{n-m}. \quad (4)$$

If \mathcal{D}_0 expands to the whole plane and both $n, F_0 \rightarrow \infty$ in such a way that $\frac{n}{F_0} \rightarrow \rho$, which is a positive constant, we get

$$\lim p_m = \frac{(\rho F)^m}{m!} e^{-\rho F}. \quad (5)$$

The right-hand side of (5) is the probability function of the Poisson distribution; it depends only on the product ρF , which is called the parameter of the distribution. This probability model for points in the plane is said to be a homogeneous planar Poisson point process of intensity ρ . In the following, we simplify it as Poisson point process.

Lemma 3.3. Let \mathcal{A}_0 be a fixed convex set of area F_0 and perimeter L_0 , and let \mathcal{A}_1 be a convex set of area F_1 and perimeter L_1 . \mathcal{A}_1 is randomly dropped in the plane in such a way that it intersects with \mathcal{A}_0 . The probability that a randomly selected point $P \in \mathcal{A}_0$ is covered by \mathcal{A}_1 is given by

$$p(P \in \mathcal{A}_1) = \frac{2\pi F_1}{2\pi(F_0 + F_1) + L_0 L_1}. \quad (6)$$

Lemma 3.4. Let \mathcal{A}_0 and \mathcal{A}_1 be two fixed convex set of area F_0, F_1 and perimeter L_0, L_1 , and $\mathcal{A}_0 \subseteq \mathcal{A}_1$. Let \mathcal{A}_2 be a convex set of area F_2 and perimeter L_2 , randomly dropped in the plane in such a way that it intersects with \mathcal{A}_1 . The probability that it intersects with \mathcal{A}_0 is given by

$$p(\mathcal{A}_0 \cap \mathcal{A}_2 \neq \emptyset \mid \mathcal{A}_1 \cap \mathcal{A}_2 \neq \emptyset) = \frac{2\pi(F_0 + F_2) + L_0 L_2}{2\pi(F_1 + F_2) + L_1 L_2}. \quad (7)$$

For more detailed proofs of Lemmas 3.1, 3.2, 3.3, and 3.4 in [23].

4 EXPECTED COVERAGE RATIO UNDER STOCHASTIC DISTRIBUTION MODELS

4.1 Expected Coverage Ratio on a Plane

Theorem 4.1. Let \mathcal{A}_f be an FoI of area F_f and perimeter L_f on a plane, and let every sensor \mathcal{A}_s have the same sensing radius r . N sensors are stochastically placed on the plane in such a way that it intersects with \mathcal{A}_f according to the PP3 model or the SP3 model. The expected coverage ratio $E(f_c)$ of the FoI \mathcal{A}_f is given by

$$1 - \left(1 - \frac{2\pi^2 r^2}{2\pi(\pi r^2 + F_f) + 2\pi r L_f}\right)^N. \quad (8)$$

Proof. Please refer to the online supplemental material for the detailed proof of Theorem 4.1. The notations are listed in Table 2. \square

Corollary 4.1. Let \mathcal{A}_f be an FoI of area F_f and perimeter L_f on a plane. Let the distribution of the sensors with sensing radius r be the PP3 model or the SP3 model with intensity λ . The expected coverage ratio $E(f_c)$ of the FoI \mathcal{A}_f is as follows:

TABLE 2
Notations and Terms in Section 4

Symbol	Definition
\mathcal{A}_f	A field of interest (FoI);
F_f	The area of \mathcal{A}_f ;
L_f	The perimeter of \mathcal{A}_f ;
\mathcal{A}_s	A sensor;
r	The sensing range of a sensor;
$E(f_c)$	The expected coverage ratio;
θ	The angle between the slant and the xOy plane;
p	The probability.

$$1 - \left(1 - \frac{2\pi^2 r^2}{2\pi(\pi r^2 + F_f) + 2\pi r L_f}\right)^{\lambda(F_f + L_f r + \pi r^2)} \quad (9)$$

Proof. Please refer to the online supplemental material for the detailed proof of Corollary 4.1. \square

4.2 Expected Coverage Ratio on a Slant

Theorem 4.2. Let \mathcal{A}_f be an FoI of area F_f and perimeter L_f on a slant. Let the distribution of the sensors with sensing radius r be the SP3 model with intensity λ . The expected coverage ratio $E(f_c)$ of the FoI \mathcal{A}_f is as follows:

$$1 - \left(1 - \frac{2\pi^2 r^2}{2\pi(\pi r^2 + F_f) + 2\pi r L_f}\right)^{\lambda(F_f + L_f r + \pi r^2)} \quad (10)$$

Proof. Please refer to the online supplemental material for the detailed proof of Theorem 4.2. \square

Lemma 4.1. For any slant in reference system, if its included angle with the xOy plane is θ , the ratio between the area of any convex area and its Z-projection convex area is a constant. Its value equals to $\sec \theta$.

Lemma 4.1 can be immediately obtained from trigonometric function.

Theorem 4.3. Let \mathcal{A}_f be an FoI of area F_f and perimeter L_f on a slant whose equation can be expressed as $z = ax + by + c$. Let the distribution of the sensors with sensing radius r be the PP3 model with intensity λ . The expected coverage ratio $E(f_c)$ of the FoI \mathcal{A}_f is as follows:

$$1 - \left(1 - \frac{2\pi^2 r^2}{2\pi(\pi r^2 + F_f) + 2\pi r L_f}\right)^{\lambda \cos \theta (F_f + L_f r + \pi r^2)} \quad (11)$$

where

$$\theta = \arccos\left(\frac{1}{\sqrt{a^2 + b^2 + 1}}\right) \quad 0 \leq \theta < \frac{\pi}{2} \quad (12)$$

Proof. Please refer to the online supplemental material for the detailed proof of Theorem 4.3. \square

4.3 Results for General Complex Surface

We simplify the complex surface into many small triangles as many small slants. From this, we are able to obtain an approximate value for the coverage ratio when sensors are stochastically deployed. Let \mathcal{A}_f be the FoI with area F_f and perimeter L_f . We divide \mathcal{A}_f into many small pieces of triangle \mathcal{A}_i , with area F_i and perimeter L_i , where

i varies from 1 to n . We model the sensing area of the sensor as a sphere with radius r . Let \mathcal{A}_s be the sensing region of the sensor with area $F_s = \pi r^2$ and perimeter $L_s = 2\pi r$. In this paper, we assume that the variations in the surface are not significant within the sensing area of a single sensor. As mentioned, we discuss two sensor distribution models separately.

Theorem 4.4 (For Space Surface Poisson Point Process Model). Let the sensor distribution be SP3 on a general complex surface. The probability that a randomly chosen point P in \mathcal{A}_f is covered by the sensor is given by

$$p(P \in \mathcal{A}_s) = \frac{2\pi^2 r^2}{2\pi(\pi r^2 + F_f) + 2\pi r L_f} \quad (13)$$

Proof. Please refer to the online supplemental material for the detailed proof of Theorem 4.4. \square

Corollary 4.2. Let the sensor distribution be SP3 with intensity λ on a general complex surface, the expected coverage ratio $E(f_c)$ of an FoI \mathcal{A}_f with area F_f and perimeter L_f is as follows:

$$1 - \left(1 - \frac{2\pi^2 r^2}{2\pi(\pi r^2 + F_f) + 2\pi r L_f}\right)^{\lambda(F_f + L_f r + \pi r^2)} \quad (14)$$

Proof. Please refer to the online supplemental material for the detailed proof of Corollary 4.2. \square

Theorem 4.5 (For Planar Surface Poisson Point Process Model). Let the sensor distribution be PP3 on a general complex surface. The probability that a randomly chosen point P in \mathcal{A}_f is covered by the sensor is given by

$$\sum_i \frac{F_i}{F_f} \frac{2\pi^2 r^2}{2\pi(\pi r^2 + F_i) + 2\pi r L_i} \frac{(F_i + L_i r + \pi r^2) \cos \theta_i}{F'_f + L_f r + \pi r^2} \quad (15)$$

where θ_i is the included angle between \mathcal{A}_i slant and xOy plane of the reference system and F'_f is the area of Z-projection of \mathcal{A}_f .

Proof. Please refer to the online supplemental material for the detailed proof of Theorem 4.5. \square

Corollary 4.3. Let the sensor distribution be PP3 with intensity λ on a general complex surface; the expected coverage ratio $E(f_c)$ of an FoI \mathcal{A}_f with area F_f and perimeter L_f is as follows:

$$E(f_c) = 1 - \left(1 - \sum_i \frac{F_i}{F_f} \frac{2\pi^2 r^2}{2\pi(\pi r^2 + F_i) + 2\pi r L_i} \frac{(F_i + L_i r + \pi r^2) \cos \theta_i}{F'_f + L_f r + \pi r^2}\right)^{\lambda(F'_f + L_f r + \pi r^2)} \quad (16)$$

Proof. Please refer to the online supplemental material for the detailed proof of Corollary 4.3. \square

We can easily verify that the results of PP3 and SP3 are the same, and match precisely the previous result when the surface is an ideal plane, i.e., $\theta_i = 0$, $F'_f = F_f = \sum_i F_i$.

Our analysis provides the methods to compute the expected coverage ratio when a given number of sensors are randomly scattered on the 3D surface. These methods could also give underlying insights for determining the

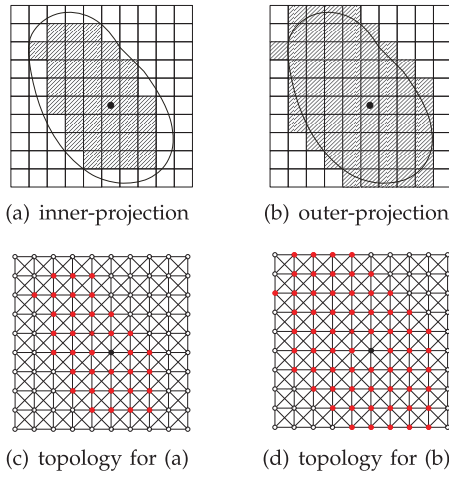


Fig. 5. An example to show the difference between inner-projection and outer-projection through top view (a,b) and topology graphs (c,d).

appropriate number of sensors that achieves a required coverage ratio before deployment.

5 DETERMINISTIC DEPLOYMENT PROBLEM

The original optimum surface coverage problem is a difficult continuous problem. So we convert it to a discrete problem and then relate the results back to the original continuous problem. We prove the hardness of the problem and propose three algorithms offering approximate solutions.

Definition 5.1. A Partition is a set defined on a surface S : $\eta = \{S_1, S_2, \dots, S_k\}$ which satisfies: $S_i \subseteq S (i = 1 \dots k)$, $S_i \cap_{i \neq j} S_j = \emptyset$, and $\bigcup_{i=1}^k S_i = S$. Let \mathcal{P} be the set of all the partitions. Use $\text{Gran}(\eta) = \max_{i=1 \dots k} \{\|S_i\|\}$ to denote granularity of partition η . The relation \preceq is a partial semiorder relation in $\mathcal{P} \times \mathcal{P}$: $\eta_i \preceq \eta_j$ if and only if η_j is a finer partition than η_i . The function $h: \eta \rightarrow 2^n$ is a function defined on partition η . Its value is a partition set that is covered by a sensor, where the independent variable is the position of the sensor. The function $h^*: 2^n \rightarrow 2^n$ is a set function defined as $L \subseteq \eta$, $h^*(L) = \bigcup_{i \in L} h(i)$.

Definition 5.2. The topology graph of partition η is a graph $G(V, E)$, where a vertex v_i corresponds to S_i in partition η . An edge is added between vertices v_i and v_j if S_i and S_j are neighbors to each other by sharing their border or a common point. Figs. 5c and 5d show the corresponding topology graphs of Figs. 5a and 5b. The distance between two pieces in a partition is defined as the length of the shortest path between the corresponding vertices. For a sensor positioned at any piece S_i , its sensing radius R is defined as the longest distance from v_i to any other vertex within its sensing area whereas its sensing diameter D is defined as the longest distance between any two vertices within its sensing area.

Definition 5.3. A feasible solution to the partition coverage problem is defined as a set L satisfying $L \subseteq \eta$ and $h^*(L) \supseteq \eta$. The Optimum Partition Coverage Problem (OPCP) is defined as: minimize $|L|$, L is a feasible solution.

To solve the OSCP, we have converted the problem from its original continuous form to a discrete one. If function g in the continuous version and function h in the

discrete one are correlated, we can establish a relationship between their corresponding solutions as specified in the following lemmas.

Lemma 5.1. For every $S_i \in$ partition η , if there exists a point k in S_i to satisfy $g(k) \supseteq h(S_i)$, any feasible solutions to the discrete version of the problem will be a feasible solution to the continuous version; For any point k in S_i , if $h(S_i) \supseteq g(k)$, any feasible solutions to the continuous version of the problem will be a feasible solution to the discrete version.

In fact, due to the impact of the surface, the coverage area of a sensor is no longer a unit disk. The function g is determined by the characteristic of the surface. For the discrete problem, there are two mechanisms to deal with the boundary: inner-projection and outer-projection. The values of an inner-projection function are all the pieces located within the coverage area, i.e., $g(k) \supseteq h(S_i)$. On the other hand, the values of an outer-projection function include that of inner-projection plus all the pieces located at the boundary, i.e., $h(S_i) \supseteq g(k)$. Figs. 5a and 5b show the instances of the inner-projection and outer-projection for the same function g . To satisfy the first part of Lemma 5.1, we focus on the inner-projection function from now on to ensure that our results for the discrete problem are applicable to the continuous problem.

Lemma 5.2. Let S_{opt} be the solution to the OSCP, η_{opt} be the solution to the OPCP under partition η , and function h be an inner-projection of function g in the OSCP. Let $\eta^1, \eta^2, \dots, \eta^i, \dots$ be a sequence of partitions with $\eta^i \preceq \eta^{i+1}$ and $\lim_{i \rightarrow \infty} \text{Gran}(\eta^i) = 0$. We have η_{opt}^i is monotonically decreasing as i increases and $\lim_{i \rightarrow \infty} \eta_{opt}^i = S_{opt}$.

The above two lemmas guarantee that when the partition is fine enough, the result of the OPCP can approximate the result of the OSCP precisely. To show the hardness of the OPCP, we prove that a special case of the OPCP, called optimum rectangular grid coverage (ORGC) problem, is NP-complete. The ORGC problem limits the shape of the sensing area and the shape of the partition in the original partition coverage problem. Since the ORGC problem is a special case of OPCP, the latter is also NP-complete.

5.1 The Hardness of the ORGC Problem

Definition 5.4. The optimum rectangular grid coverage problem is defined as: we consider an $N \times N$ grid \mathcal{G} , where each pane $E_{(i,j)} \in \mathcal{G}$ is associated with four numbers to specify its coverage rectangle $\mathcal{O}_{(i,j)}$. The ORGC problem is to find a subset \mathcal{G}' that minimizes $|\mathcal{G}'|$ while satisfying: $\{\bigcup_{E_{(i,j)} \in \mathcal{G}'} \mathcal{O}_{(i,j)}\} \supseteq \mathcal{G}$.

Theorem 5.1. The ORGC problem is NP-complete.

Proof. Planar 3SAT (P3SAT) is 3SAT restricted to formulae B such that $G(B)$ is planar. P3SAT is NP-complete [19]. We divide the procedure of reducing from P3SAT into two steps. Step I, we show that there is a polynomial time computable function f which converts an instance in P3SAT to an instance in ORGC. Step II, we prove that:

$$w \in P3SAT \iff f(w) \in ORGC, \quad (17)$$

where w is an instance in P3SAT.

Please refer to the online supplemental material for the detailed proof of Theorem 5.1. \square

5.2 Approximation Algorithms for Solving the Optimum Partition Coverage Problem (OPCP)

Since the OPCP is NP-complete, we propose three algorithms to solve it approximately. Algorithm 1 is a greedy algorithm. It selects a position that can increase the covered region the most.

Algorithm 1: Greedy Algorithm for OPCP

Input : Partition \mathcal{P} , function h of every pieces S_i
Output: A subset \mathcal{P}' of \mathcal{P}

```

1  $\mathcal{P}' \leftarrow \emptyset; \mathcal{C} \leftarrow \emptyset;$ 
2 while  $\mathcal{C} \not\supseteq \mathcal{P}$  do
3    $m \leftarrow 0, x \leftarrow 0;$ 
4   for every  $S_i$  in  $\mathcal{P} - \mathcal{P}'$  do
5     if  $|h(S_i) - \mathcal{C}| > m$  then
6        $m \leftarrow |h(S_i) - \mathcal{C}|; x \leftarrow i;$ 
7     end
8   end
9    $\mathcal{P}' \leftarrow \mathcal{P}' \cup \{S_x\}; \mathcal{C} \leftarrow \mathcal{C} \cup h(S_x);$ 
10 end

```

Theorem 5.2. *Algorithm 1 is an $O(|\mathcal{P}|^2)$ time $\log(|\mathcal{P}|)$ -approximation algorithm.*

Proof. Please refer to the online supplemental material for the detailed proof of Theorem 5.2. \square

Actually, if we assume the diameter of the sensing area is D as defined in Definition 5.2, then we can make use of the “shifting strategy” proposed in [9] to develop an polynomial-time approximation scheme (PTAS) algorithm to solve it. The approximation ratio can be $(1 + \frac{1}{\epsilon})^2$. Since it is based on divide-and-conquer idea, it can be easily implemented in a distributed manner.

The main idea of Algorithm 2 is to divide the FoI into vertical strips of width D . These strips are then considered in groups of l consecutive strips resulting in strips of width $l \times D$ each. For any fixed division into strips of width D , there are l different ways of partitioning FoI into strips of width $l \times D$. These partitions can be ordered such that each can be derived from the previous one by shifting it to the right over distance D . We use the same method to solve the subproblem and output the union of all positions. For l different shifting partitions, we select the optimum result as the final result.

The main framework and some symbols can refer to [9]. Especially, Algorithm 2 includes two alternative parts: Algorithm 2(a) and Algorithm 2(b). The most pseudocodes of these two algorithms are the same. The difference is that Algorithm 2(a) only carries out Line 7 but not Line 8 and Algorithm 2(b) only operates Line 8 but not Line 7.

Theorem 5.3. *Algorithm 2(a) is an $O(\frac{|\mathcal{P}|}{D^2} \times 2^{l^2 D^2})$ time $(1 + \frac{1}{l})^2$ -approximation algorithm.*

Proof. Please refer to the online supplemental material for the detailed proof of Theorem 5.3. \square

Although the performance ratio looks fine, it may be not practical in real environments because even $l = 1$ is a big

cost since D is often larger than five. We sacrifice some accuracy to reduce the cost of calculation. This brings us to Algorithm 2(b). It mixes the core idea in Algorithm 1 and Algorithm 2(a) and simply uses the greedy algorithm (Line 8 in Algorithm 2) instead of the brute-force algorithm (Line 7 in Algorithm 2). It can still be implemented in a distributed manner. We call it Algorithm 2(b).

Algorithm 2: Approximation Algorithm for OPCP

Input : Partition \mathcal{P} , the function h of every pieces S_i

Output: A subset \mathcal{P}' of \mathcal{P}

```

1 Divide  $\mathcal{P}$  into vertical strips to generate  $l$  shifting
  partitions  $\eta^1, \eta^2, \dots, \eta^l;$ 
2 for each shifting partition  $\eta^i$  do
3   for each strip group  $\eta_j^i \in \eta^i$  do
4     Divide  $\eta_j^i$  into horizontal strips to generate
       $l$  shifting partitions  $S\eta^1, S\eta^2, \dots, S\eta^l;$ 
5     for each shifting partition  $S\eta^u$  do
6       for each strip group  $S\eta_v^u \in S\eta^u$  do
7         Algorithm 2(a): Using brute-force
          algorithm to solve the subproblem
           $S\eta_v^u$  and let the result be  $R_v^u;$ 
8         Algorithm 2(b): Using greedy
          algorithm to solve the subproblem
           $S\eta_v^u$  and let the result be  $R_v^u;$ 
9       end
10       $R^u \leftarrow \bigcup_{v=1}^{\lceil \frac{m}{l \times D} \rceil} R_v^u;$ 
11     end
12      $R_j^i \leftarrow \min_{|R^u|} R^u;$ 
13   end
14    $R^i \leftarrow \bigcup_{j=1}^{\lceil \frac{n}{l \times D} \rceil} R_j^i;$ 
15 end
16  $\mathcal{P}' \leftarrow \min_{|R^i|} R^i;$ 

```

Theorem 5.4. *Algorithm 2(b) is an $O(|\mathcal{P}|l^4 D^2)$ time $\log(l^2 D^2) \times (1 + \frac{1}{l})^2$ -approximation algorithm.*

Proof. Please refer to the online supplemental material for the detailed proof of Theorem 5.4. \square

6 PERFORMANCE EVALUATION

The main purpose of the evaluation is to: 1) point out the limitation of the traditional methods, 2) verify our derived results, and 3) make comparisons of the three proposed algorithms in a comprehensive manner.

We utilize Terragen [2], a professional terrain generating tool to simulate surface, and the widely used “Ridged Perlin Noise” to generate a natural, ridged landscape. Glaciation is a widely used parameter to measure the steepness of a terrain [2]. A low Glaciation generates a smoothly flat terrain as shown in Fig. 6a. On the contrary, a high Glaciation generates a sharply fluctuant terrain as shown in Fig. 6b. We use triangularization to partition a surface for our evaluation. Fig. 6c depicts surface triangularization.

There are several methods for covering the FoI if the FoI is an ideal 2D plane. The typical one is the triangle pattern [14]. Thus, we take this method as the representative pattern for performance evaluation. Six different terrains

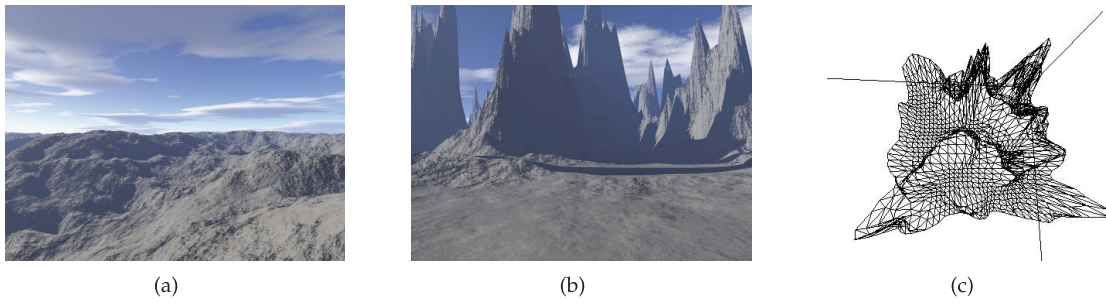


Fig. 6. (a) Terrain1 with Glaciation = 20 generated by Terragen [2]. (b) Terrain2 with Glaciation = 100. (c) Terrain2 after triangularization (Top view).

are generated, whose Glaciation is set 0, 20, 40, 60, 80, and 100, respectively. All sensors can be only deployed on the surface. In this simulation, the size of the FoI is set to be $1,920 \times 1,920 \text{ m}^2$. The height range is from 300 m to 2,000 m and the sensing radius is 30 m. Finally, we calculate the coverage ratio. Fig. 7 presents the performance of the typical triangle pattern. The number of sensors is set to satisfy the minimum value for achieving full coverage (the coverage ratio is 1) when $Glaciation = 0$. When the parameter Glaciation increases, the coverage ratio decreases quickly. It drops to about 60 percent when $Glaciation = 100$. Hence, the conventional triangle pattern does not work well on a complex surface. It is necessary to find new methods to cover the complex surface.

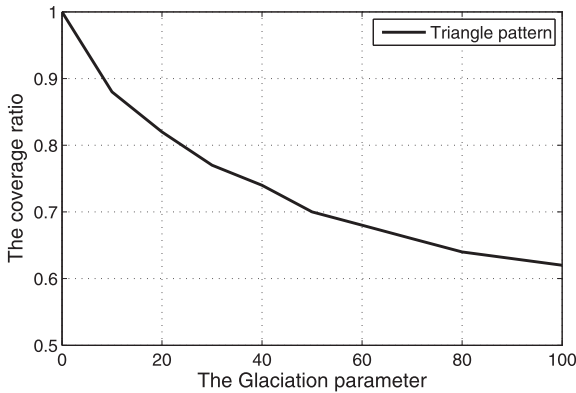


Fig. 7. The sensors fully cover a plane FoI ($Glaciation = 0$). But the coverage ratio drops when Glaciation increases. This simulation demonstrates that it is necessary to study the surface coverage problem.

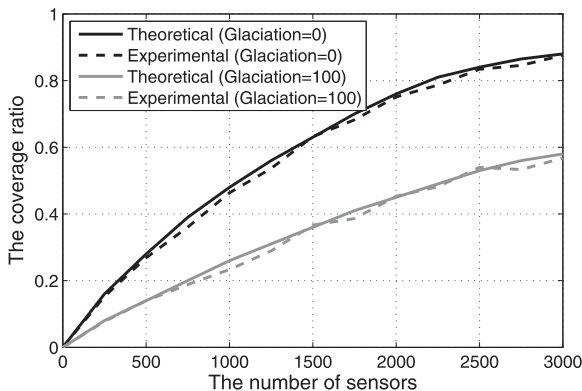


Fig. 8. The expected coverage ratio in stochastic distribution case. We compare the theoretical value calculated by our proposed method and the experimental value obtained in the simulation.

Fig. 8 shows the coverage ratio under stochastic distribution. The solid lines present the theoretical results calculated by the proposed methods in Section 4. And the dash lines present the experimental results obtained by our simulation, which we stochastically deploy sensors on the surface and do the statistics of the coverage ratio. We find that the theoretical results match the experimental results precisely, no matter the Glaciation is low or high. Fig. 8 demonstrates the validity of our method to calculate the coverage ratio under stochastic distribution on complex surface.

Fig. 9 compares the results of the three proposed algorithms under deterministic deployment. We utilize a square partition in our experiment because the terrain file is a dot matrix and can be easily converted to a square partition. The FoI is a $N \times N$ grid, where N is the distance measured by partitions. The X -axis is the side length of the FoI and the Y -axis means how many sensors are needed to have a complete coverage (coverage ratio is 1) of the FoI. The performance of the simple greedy algorithm provides the best result, which demands the minimum number of sensors for complete coverage. Algorithm 2(a) has the best theoretical performance bound when l (refer to Section 5.2) is large enough. Unfortunately, the time complexity is exponential as l increases. Thus, it can only be executed effectively when $l = 1$ and $D \leq 5$ (refer to Definition 5.2). However, the small D implicates that the size of the partition is large. We must guarantee that the partition is detailed enough to get a precise solution to the original OSCP as stated in Lemma 5.2. In Fig. 9, D is set to be 3 so that we can compare Algorithm 2(a) with other algorithms.

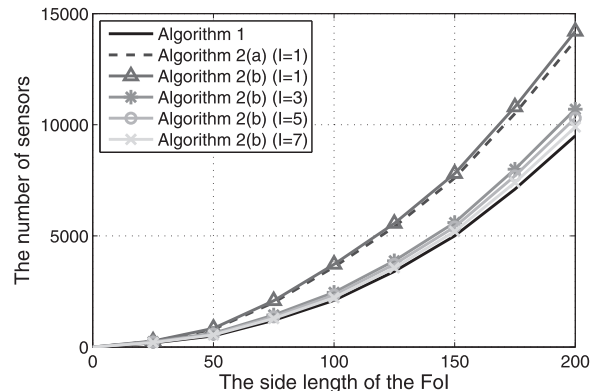


Fig. 9. In deterministic deployment case, the minimum number of sensors satisfies the full coverage of an FoI with given side length. The results are obtained by our proposed algorithms when sensing diameter $D = 3$.

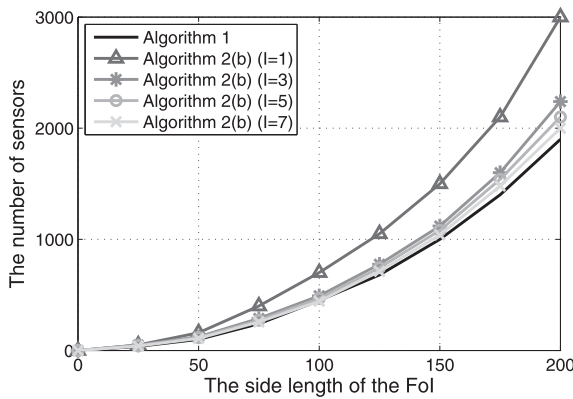


Fig. 10. In deterministic deployment case, the minimum number of sensors satisfies the full coverage of an FoI with given side length. The results are obtained by our proposed algorithms when sensing diameter $D = 7$.

We find that the results of Algorithm 2(a) and 2(b) ($l = 1$) is close. Furthermore, the number of sensors decreases when l increases for Algorithm 2(b).

The experiment of Fig. 10 is similar to Fig. 9, but the sensing diameter is changed to $D = 7$. Fig. 10 also compares the three proposed algorithms. The performance of Algorithm 1 is still the best. Note that Algorithm 2(a) and Algorithm 2(b) can be implemented in a distributed manner, and we propose Algorithm 2(b) because the calculation cost of Algorithm 2(a) is too large.

The results tell us that algorithm 1 is the best choice. Although its theoretical performance bound is not very acceptable, its average approximation ratio is precise enough.

7 DISCUSSIONS

In this section, we discuss some practical issues.

1. *Surface is not a single-valued function (i.e., not convex).* Note that our solution only depends on a partition of the surface. If we have proper expressions of the surface when it is not a single-valued function, we can partition it and our solution can still be applied.
2. *The errors between a smooth surface and a surface with triangles.* Due to discrepancy between a smooth surface and a triangulated surface, unavoidable errors that occur when converting a smooth surface into a triangulated one are minimized when the triangles are small. Since geographic information systems (GIS) provide data in a dot matrix, accuracy is lost in this data storage system, and not in the calculation process.
3. *Relationship between surface parameter and coverage ratio.* After a survey of the current surface parameters in the GIS, we have not found any relative parameters. The impact on coverage ratio is the ratio of the area to the projective area. In general, a terrain with more mountains and densely populated with mountains will have a relatively poor coverage ratio.

8 CONCLUSIONS AND FUTURE WORK

We have proposed a new model for the coverage problem called surface coverage to better capture real-world application challenges. Two problems pertaining to surface

coverage were in focus: the expected coverage ratio with stochastic deployment and the optimal deployment strategy with planned deployment. Comprehensive simulation experiments show that though the performance bound of the greedy algorithm is not the best, it often outperforms the other two algorithms. To our best knowledge, this is the first attempt to describe and resolve the surface coverage problem in WSNs.

Future research can be carried out following many directions. For instance, our research considers only static sensors. Mobile sensors for surface coverage are worthy to further study. Moreover, the connectivity problem is still an open problem in surface coverage domain.

ACKNOWLEDGMENTS

This research was supported by US National Science Foundation of China under grant no. 60773091, 973 Program of China under grant no. 2006CB303000, 863 Program of China under grant no. 2006AA01Z247, Innovation program of SJTU under grant no. Z-030-022, Hong Kong RGC Grants HKUST617908 and HKBU 1/05C, the Key Project of China NSFC grant 60533110. Our shepherd, Jin-Yi Cai, Xiang-Yang Li, Dong Xuan, Ten H. Lai, and Lionel M. Ni gave us highly valuable comments.

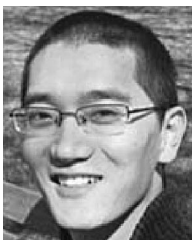
REFERENCES

- [1] <http://fiji.eecs.harvard.edu/Volcano/>, 2013.
- [2] <http://www.planetside.co.uk/terragen/>, 2013.
- [3] X. Bai, D. Xuan, Z. Yun, T.H. Lai, and W. Jia, "Complete Optimal Deployment Patterns for Full-Coverage and K-Connectivity ($k \leq 6$) Wireless Sensor Networks," *Proc. ACM MobiHoc*, pp. 401-410, 2008.
- [4] P. Balister, B. Bollobas, A. Sarkar, and S. Kumar, "Reliable Density Estimates for Coverage and Connectivity in Thin Strips of Finite Length," *Proc. ACM MobiCom*, pp. 75-86, 2007.
- [5] Y. Bejerano, "Simple and Efficient K-Coverage Verification without Location Information," *Proc. IEEE INFOCOM*, pp. 291-295, Apr. 2008.
- [6] M. Cardei, M. Thai, Y. Li, and W. Wu, "Energy-Efficient Target Coverage in Wireless Sensor Networks," *Proc. IEEE INFOCOM*, vol. 3, pp. 1976-1984, Mar. 2005.
- [7] A. Chen, S. Kumar, and T.H. Lai, "Designing Localized Algorithms for Barrier Coverage," *Proc. ACM MobiCom*, pp. 63-74, 2007.
- [8] P. Corke, S. Hrabar, R. Peterson, D. Rus, S. Saripalli, and G. Sukhatme, "Autonomous Deployment and Repair of a Sensor Network Using an Unmanned Aerial Vehicle," *Proc. IEEE Int'l Conf. Robotics and Automation (ICRA)*, vol. 4, pp. 3602-3608, May 2004.
- [9] D.S. Hochbaum and W. Maass, "Approximation Schemes for Covering and Packing Problems in Image Processing and Vlsi," *J. ACM*, vol. 32, no. 1, pp. 130-136, 1985.
- [10] C.-F. Huang, Y.-C. Tseng, and L.-C. Lo, "The Coverage Problem in Three-Dimensional Wireless Sensor Networks," *Proc. IEEE Global Telecomm. (GLOBECOM)*, vol. 5, pp. 3182-3186, Nov./Dec. 2004.
- [11] R. Iyengar, K. Kar, and S. Banerjee, "Low-Coordination Topologies for Redundancy in Sensor Networks," *Proc. ACM MobiHoc*, pp. 332-342, 2005.
- [12] M. Jin, G. Rong, H. Wu, L. Shuai, and X. Guo, "Optimal Surface Deployment Problem in Wireless Sensor Networks," *Proc. IEEE INFOCOM*, pp. 2345-2353, 2012.
- [13] K. Kar and S. Banerjee, "Node Placement for Connected Coverage in Sensor Networks," *Proc. WiOpt*, pp. 1-10, Apr. 2003.
- [14] R. Kershner, "The Number of Circles Covering a Set," *Am. J. Math.*, 1939.
- [15] L. Kong, D. Jiang, and M. Wu, "Optimizing the Spatio-Temporal Distribution of Cyber-Physical Systems for Environment Abstraction," *Proc. IEEE 30th Int'l Conf. Distributed Computing Systems (ICDCS)*, pp. 179-188, 2010.

- [16] S. Kumar, T.H. Lai, and A. Arora, "Barrier Coverage with Wireless Sensors," *Proc. ACM MobiCom*, pp. 284-298, 2005.
- [17] L. Lazos and R. Poovendran, "Stochastic Coverage in Heterogeneous Sensor Networks," *ACM Trans. Sensor Network*, vol. 2, no. 3, pp. 325-358, 2006.
- [18] X.-Y. Li, P.-J. Wan, and O. Frieder, "Coverage in Wireless Ad Hoc Sensor Networks," *IEEE Trans. Computers*, vol. 52, no. 6, pp. 753-763, June 2003.
- [19] D. Lichtenstein, "Planar Formulae and Their Uses," *SIAM J. Computing*, vol. 11, no. 2, pp. 329-343, 1982.
- [20] B. Liu, P. Brass, O. Dousse, P. Nain, and D. Towsley, "Mobility Improves Coverage of Sensor Networks," *Proc. ACM MobiHoc*, pp. 300-308, 2005.
- [21] L. Liu and H. Ma, "On Coverage of Wireless Sensor Networks for Rolling Terrains," *IEEE Trans. Parallel and Distributed Systems*, vol. 23, no. 1, pp. 118-125, Jan. 2012.
- [22] S. Meguerdichian, F. Koushanfar, M. Potkonjak, and M. Srivastava, "Coverage Problems in Wireless Ad-Hoc Sensor Networks," *Proc. IEEE INFOCOM*, vol. 3, pp. 1380-1387, 2001.
- [23] L.A. Santalo, *Integral Geometry and Geometric Probability*. Addison-Wesley, 1976.
- [24] W.W.V. Srinivasan and K.-C. Chua, "Trade-Offs between Mobility and Density for Coverage in Wireless Sensor Networks," *Proc. ACM MobiCom*, pp. 39-50, 2007.
- [25] X. Wang, G. Xing, Y. Zhang, C. Lu, R. Pless, and C. Gill, "Integrated Coverage and Connectivity Configuration in Wireless Sensor Networks," *Proc. ACM First Int'l Conf. Embedded Networked Sensor Systems (SenSys)*, pp. 28-39, 2003.
- [26] M. Watfa and S. Commuri, "A Coverage Algorithm in 3d Wireless Sensor Networks," *Proc. IEEE First Int'l Symp. Wireless Pervasive Computing (PerCom)*, Jan. 2006.
- [27] H. Zhou, H. Wu, S. Xia, M. Jin, and N. Ding, "A Distributed Triangulation Algorithm for Wireless Sensor Networks on 2D and 3D Surface," *Proc. IEEE INFOCOM*, pp. 1053-1061, 2011.



Linghe Kong received the BE degree in the Automation Department from Xidian University, China, in 2005, and the Dipl Ing degree in telecommunication from TELECOM SudParis (ex. INT), France, in 2007. He is currently working toward the PhD degree in the Department of Computer Science and Engineer in Shanghai Jiao Tong University with Prof. Min-You Wu. His research interests include the area of wireless sensor networks and cyber-physical systems. He is a member of the IEEE.



Mingchen Zhao received the bachelor of engineering and master of engineering degrees from the Computer Science and Engineering Department of Shanghai Jiao Tong University, under the supervision of Prof. Min-You Wu. He is working toward the PhD degree in the Computer and Information Science Department of the University of Pennsylvania. Supervised by Prof. Andreas Haeberlen, he mainly works on security problems in distributed systems.



Xiao-Yang Liu received the BE degree in computer science in Huazhong University of Science and Technology, China, in 2009. He is currently working toward the PhD degree in Department of Computer Science and Engineer in Shanghai Jiao Tong University with Prof. Min-You WU. His research interests include the area of wireless sensor networks.



Jialiang Lu received the master and PhD degrees in INSA Lyon, France, in 2008. He is currently an assistant researcher in the Department of Computer Science and Engineer at Shanghai Jiao Tong University. His research interests include the area of wireless sensor networks. He is a member of the IEEE.



Yunhuai Liu received the BS degree from the Computer Science and Technology Department of Tsinghua University in July, 2000. Then he got his first job in Hewlett Packard in Beijing, China, as a system engineer. After nearly three years of working with HP, he began to pursuit the PhD degree at the Computer Science Department in Hong Kong University of Science and Technology. In July 2008, he passed the final defense of PHD. After that, he worked as an research

assistant professor in Hong Kong University of Science and Technology. In 2010 August, he joined the Institute of Advanced Computing and Digital Engineering, Shenzhen Institutes of Advanced echnology, Chinese Academy of Sciences, to start a new career. He is now an associate professor in Third Research Institute of Ministry of Public Security in Shanghai. He is a member of the IEEE.



Min-You Wu (S'84-M'85-SM'96) received the MS degree from the Graduate School of Academia Sinica, Beijing, China, in 1981 and the PhD degree from Santa Clara University, California, in 1984. He is a professor in the Department of Computer Science and Engineering at Shanghai Jiao Tong University and a research professor with the University of New Mexico. He serves as the chief scientist at Grid Center of Shanghai Jiao Tong University. His research interests include grid computing, wireless networks, sensor networks, multimedia networking, parallel and distributed systems, and compilers for parallel computers. He is a senior member of the IEEE.



Wei Shu (M'90-SM'99) received the PhD degree from the University of Illinois at UrbanaCChampaign. She was with the Yale University, New Haven, Connecticut, the State University of New York at Buffalo, and the University of Central Florida, Orlando. She is currently an associate professor with the Department of Electrical and Computer Engineering, University of New Mexico, Albuquerque. She is also a visiting professor in

Shanghai Jiao Tong University, China. Her current research interests include resource management, multimedia networking, distributed systems, wireless networks, and sensor networks. She is a senior member of the IEEE.

► For more information on this or any other computing topic, please visit our Digital Library at www.computer.org/publications/dlib.